A Molecular Mechanics Study of Copper(II)-Catalyzed Asymmetric Diels−Alder Reactions

Robert J. Deeth* and Natalie Fey[†]

*Inorganic Computational Chemistry Group, Department of Chemistry, University of Warwick, Coventry, CV4 7AL, U.K.*

A simple molecular mechanics force field for the study of complexes important in the bis-(oxazoline) copper(II)-catalyzed Diels−Alder reaction of cyclopentadiene with acrylimide dienophiles has been developed. The parameter set has been based on the MMFF94 force field as implemented in the Molecular Operating Environment (MOE) and supplemented by available experimental and DFT calculated data. Control over the electronic preference for a square-planar complex geometry has been achieved by introducing a dummy bond. Catalyst−substrate complexes and approximate transition states have been studied by stochastic conformational searches to investigate conformational preferences and to estimate regio- and enantioselectivities based on the steric characteristics of different bis(oxazoline) ligands. While prediction of regioselectivity is reliable, factors determining enantioselectivity are more subtle, and predictions have been only moderately successful. Further computational experiments have been used to elucidate the source of some of these discrepancies.

Introduction

The development of catalytically active transition metal complexes has sparked a renaissance in organic asymmetric synthesis. Reactivity and selectivity can be considerably enhanced through metal complexation, and, unlike biomolecular catalysis, facile access to both enantiomers of catalyst, and hence product, is generally retained.[1] The development of rational design criteria for suitable transition metal/ligand complexes has benefited from the recognition of the potential reduction in the number of competing transition states due to the presence of a symmetry axis within certain complexes.[2] Topological analysis has suggested a beneficial interplay between C_2-symmetry and square-planar complexes.[3] In line with these observations, C_2-symmetrical transition metal complexes of chiral bis(oxazoline) ligands have found widespread application in the Lewis acid catalysis of a variety of synthetic transformations (described for example in refs 1 and 4), and their coordination chemistry has been reviewed.[5]

Considerable research interest has been focused on the development of suitable complexes for the homogeneous enantioselective Diels−Alder reaction of acrylimide dienophiles **1** with cyclopentadiene to give **2** in high regio- and enantioselectivity (Scheme 1), which has served as a testing ground for the development of chiral, catalytically active Lewis acids (see for example refs

Scheme 1
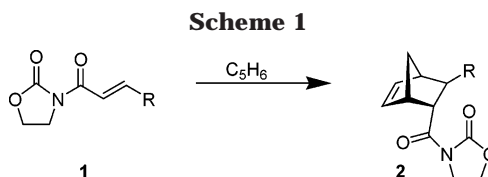
6−9). While a number of main group and transition metals have been found to catalyze this reaction, copper-(II) complexes of suitably substituted chiral bis(oxazoline) and pyridyl-bis(oxazoline) ligands have been extremely successful and hence widely investigated.[10−21]
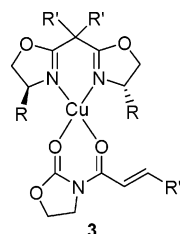
A distorted square-planar intermediate **3** has been confirmed by a combination of X-ray diffraction struc-

* Corresponding author. Fax: +44 2476 524112. E-mail: r.j.deeth@warwick.ac.uk.
† Present address: School of Chemistry, University of Bristol, BS8 1TS, U.K.
(1) Ghosh, A. K.; Mathivanan, P.; Cappiello, J. *Tetrahedron: Asymmetry* **1998**, *9*, 1.
(2) Whitesell, J. K. *Chem. Rev.* **1989**, *89*, 1581.
(3) Moberg, C. *Angew. Chem., Int. Ed.* **1998**, *37*, 248.
(4) Johnson, J. S.; Evans, D. A. *Acc. Chem. Res.* **2000**, *33*, 325.
(5) Gomez, M.; Muller, G.; Rocamora, M. *Coord. Chem. Rev.* **1999**, *193−195*, 769.

(6) Chow, I.-F.; Mak, C. C. *J. Org. Chem.* **1997**, *62*, 5116.
(7) Ghosh, A. K.; Cho, H.; Cappiello, J. *Tetrahedron: Asymmetry* **1998**, *9*, 3687.
(8) Carmona, D.; Lamata, M. P.; Oro, L. A. *Coord. Chem. Rev.* **2000**, *200−202*, 717.
(9) Hiroi, K.; Watanabe, K.; Abe, I.; Koseki, M. *Tetrahedron Lett.* **2001**, *42*, 7617.
(10) Evans, D. A.; Miller, S. J.; Lectka, T. *J. Am. Chem. Soc.* **1993**, *115*, 6460.
(11) Evans, D. A.; Murry, J. A.; Matt, P. v.; Norcross, R. D.; Miller, S. J. *Angew. Chem., Int. Ed. Engl.* **1995**, *34*, 798.
(12) Evans, D. A.; Kozlowski, M. C.; Tedrow, J. S. *Tetrahedron Lett.* **1996**, *37*, 7481.
(13) Davies, I. W.; Gerena, L.; Castonguay, L.; Senanayake, C. H.; Larsen, R. D.; Verhoeven, T. R.; Reider, P. J. *Chem. Commun.* **1996**, 1753.
(14) Davies, I. W.; Gerena, L.; Cai, D.; Larsen, R. D.; Verhoeven, T. R.; Reider, P. J. *Tetrahedron Lett.* **1997**, *38*, 1145.

tures, double-stereodifferentiation experiments, and PM3 semiempirical calculations (summarized in refs 22 and 21), and the importance of steric effects on selectivity has been illustrated by the experimental studies (vide supra). The impact of oxazoline ligand variation has been systematically investigated in a series of experimental and computational studies.[13,14,20] While this work has successfully applied the ligand field molecular mechanics (LFMM) approach to the modeling of copper(II) bis(oxazoline) aquo complexes, comprehensive conformational searching of the catalyst−substrate complexes and likely transition states was beyond the capabilities of the software used. A recent investigation has developed quantitative structure−activity relationships (QSAR) for bis(oxazoline) and phosphinooxazoline catalysts to determine the origin of the variance in experimentally observed enantiomeric excesses.[23] On the basis of semiempirically (PM3) optimized catalyst structures and systematic conformer searches, the authors used comparative molecular field analysis (CoMFA) of the copper(II)-oxazoline units to derive a suitable QSAR model, which allowed them to attribute about 70% of the observed variance to the steric field of the catalysts and to suggest structural modifications to improve catalyst performance. Interactions between the oxazoline ligands and the coordinated substrate have not been considered in this analysis.

We are planning to introduce the LFMM approach into a modern, commercially available molecular mechanics package and have chosen the Molecular Operating Environment (MOE)[24] as a suitable platform. While a variety of force fields have been developed to deal with inorganic complexes (see for example *Coord. Chem. Rev.* **2001**, 212, for a recent collection of reviews of inorganic computational chemistry), MOE currently does not contain any force fields suitable for modeling transition metal complexes. As a first step toward the planned integration of LFMM in MOE, we have extended the MMFF94 force field[25−29] to permit geometry optimizations and conformational searching of catalyst−substrate complexes and approximate transition states for a wide variety of bis(oxazoline) ligands. This force field was chosen because of the computational derivation of its parameter set,[25] the broad range of compounds parametrized,[25,28,29] and its strong performance compared to other popular force fields.[30] Extension of a commercially available package with a simple and transferable force field, capable of appropriately treating the copper(II) bis(oxazoline) catalyst system, was aimed at exploring MOE's capabilities with respect to transition metal complexes, as well as providing a versatile computational tool for the theoretical evaluation of new ligands.[31] In this publication, we present a comparison of calculated and experimentally observed regio- and enantioselectivities to assess the success of this force field approach and to analyze substituent steric effects important in determining complex geometries and hence selectivities.

Results and Discussion

A. Force Field Parametrization. The balance of electronic and steric demands of both metal ion and ligands generally determines the geometry of coordination complexes.[31−33] It is indeed one of the main reasons for the success of transition metal catalysts that small variations in any of these factors can foster significant changes in complex geometry, thus permitting stabilization of different chemical environments and hence control over the regio- and stereoselectivity of reactions.[33] A successful computational approach has to capture both electronic and steric properties of transition metal complexes at reasonable computational cost. Density functional theory (DFT) calculations have consistently produced good agreement with experimental data for transition metal complexes (see for example refs 34−37), but extensive conformational searching and the investigation of large molecular systems, as would be required for a systematic variation of bis(oxazoline) ligand steric demands, are generally not computationally viable. The application of quantum mechanical/molecular mechanical (QM/MM) hybrid approaches to transition metal complexes (see for example refs 38 and 39) has begun to pave the way toward a suitable compromise between the speed of MM and the more accurate treatment of electronic effects achieved in a QM/DFT context. However, the definition of the partitioning, embedding, and linking of areas treated at different levels of theory remains an area of active research (see for example refs 40−46) and as such is not immediately suitable as a basis for an approach accessible to the nonspecialist computational chemist.

(15) Takacs, J. M.; Lawson, E. C.; Reno, M. J.; Youngman, M. A.; Quincy, D. A. *Tetrahedron Asymmetry* **1997**, *8*, 3073.

(16) Evans, D. A.; Olhava, E. J.; Johnson, J. S.; Janey, J. M. *Angew. Chem., Int. Ed.* **1998**, *37*, 3372.

(17) Evans, D. A.; Miller, S. J.; Lectka, T.; Matt, P. v. *J. Am. Chem. Soc.* **1999**, *121*, 7559.

(18) Evans, D. A.; Johnson, J. S.; Burgey, C. S.; Campos, K. R. *Tetrahedron Lett.* **1999**, *40*, 2879.

(19) Evans, D. A.; Rovis, T.; Kozlowski, M. C.; Downey, C. W.; Tedrow, J. S. *J. Am. Chem. Soc.* **2000**, *122*, 9134.

(20) Davies, I. W.; Deeth, R. J.; Larsen, R. D.; Reider, P. J. *Tetrahedron Lett.* **1999**, *40*, 1233.

(21) Rovis, T.; Evans, D. A. *Progr. Inorg. Chem.* **2001**, *50*, 1.

(22) Evans, D. A.; Barnes, D. M.; Johnson, J. S.; Lectka, T.; Matt, P. v.; Miller, S. J.; Murry, J. A.; Norcross, R. D.; Shaugnessy, E. A.; Campos, K. R. *J. Am. Chem. Soc.* **1999**, *121*, 7582.

(23) Lipkowitz, K. B.; Pradhan, M. *J. Org. Chem.* **2003**, *68*, 4648.

(24) *Molecular Operating Environment (MOE) 2001.01*; Chemical Computing Group Inc.: Montreal, 2001.

(25) Halgren, T. A. *J. Comput. Chem.* **1996**, *17*, 490.

(26) Halgren, T. A. *J. Comput. Chem.* **1996**, *17*, 520.

(27) Halgren, T. A. *J. Comput. Chem.* **1996**, *17*, 553.

(28) Halgren, T. A.; Nachbar, R. B. *J. Comput. Chem.* **1996**, *17*, 587.

(29) Halgren, T. A. *J. Comput. Chem.* **1996**, *17*, 616.

(30) Halgren, T. A. *J. Comput. Chem.* **1999**, *20*, 730.

(31) Comba, P. *Coord. Chem. Rev.* **1993**, *123*, 1.

(32) Comba, P.; Hambley, T. W. *Molecular Modeling of Inorganic Compounds*; VCH Verlagsgesellschaft mbH: Weinheim, 1995.

(33) Cundari, T. R. *J. Chem. Soc., Dalton Trans.* **1998**, *17*, 2771.

(34) Ziegler, T. *Chem. Rev.* **1991**, *91*, 651.

(35) Ziegler, T. *Can. J. Chem.* **1995**, *73*, 743.

(36) Deeth, R. J. *Struct. Bonding* **1995**, *82*, 1.

(37) Chermette, H. *Coord. Chem. Rev.* **1998**, *178−180*, 699.

(38) Maseras, F. *Chem. Commun.* **2000**, 1821.

(39) Woo, T. K.; Margl, P. M.; Deng, L.; Cavallo, L.; Ziegler, T. *Catal. Today* **1999**, *50*, 479.

(40) Bakowies, D.; Thiel, W. *J. Phys. Chem.* **1996**, *100*, 10580.

(41) Gao, J.; Amara, P.; Alhambra, C.; Field, M. J. *J. Phys. Chem. A* **1998**, *102*, 4714.
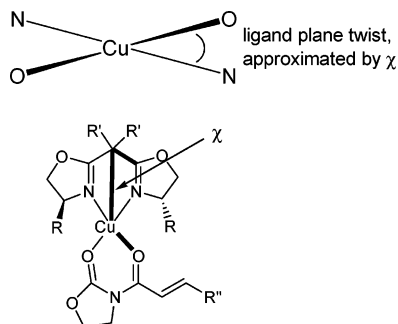
(42) Mordasini, T. Z.; Thiel, W. *Chimia* **1998**, *52*, 288.

(43) Antes, I.; Thiel, W. *J. Phys. Chem. A* **1999**, *103*, 9290.

(44) Murphy, R. B.; Philipp, D. M.; Friesner, R. A. *J. Comput. Chem.* **2000**, *21*, 1422.

(45) Reuter, N.; Dejaegere, A.; Maigret, M.; Karplus, M. *J. Phys. Chem. A* **2000**, *104*, 1720.

(46) Grigorenko, B. L.; Nemukhin, A. V.; Topol, I. A.; Burt, S. K. *J. Phys. Chem. A* **2002**, *106*, 10663.
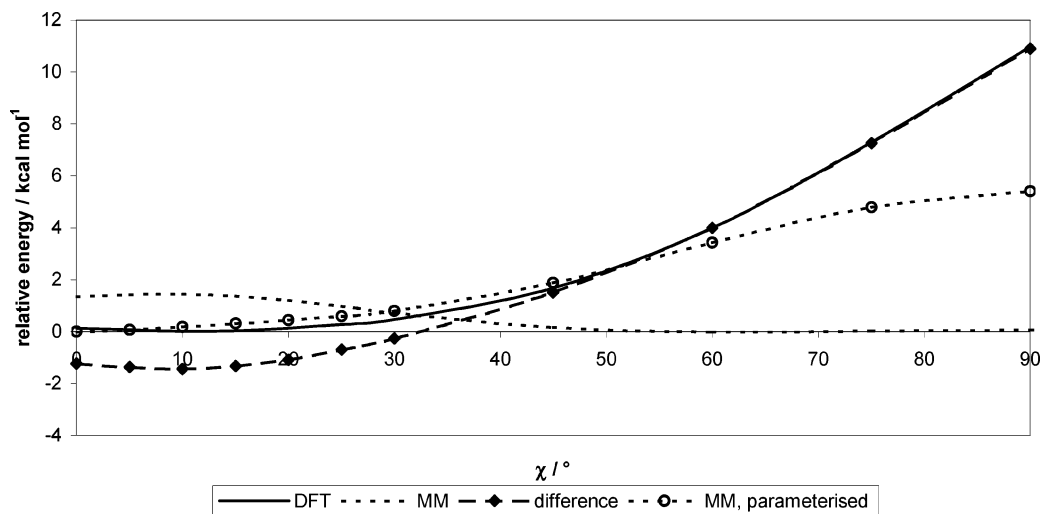
Figure 1. Schematic of ligand plane twisting (ideally, χ would be measured as the angle between two planes defined by N$-$Cu$-$N and O$-$Cu$-$O; however, MOE does not allow to define planes as part of its database analysis facility, so χ was approximated as C$-$C$\cdots$Cu$-$O).

Furthermore, with no conformational search implementation of a QM/MM hybrid yet reported and their accuracy with respect to subtle steric differences questioned,[47] we opted for a full molecular mechanical treatment for this investigation.

Due to the lack of experimentally determined structural data for the catalyst$-$substrate complex **3**, density functional theory calculations were used to help parametrize the MMFF94 force field in MOE. Both oxazoline ligands and acrylimide dienophiles **1** were treated as bidentate ligands, resulting in a four-coordinate copper-(II) center. The possibility of weak counterion coordination to yield a five-coordinate square-pyramidal copper center, as observed crystallographically for the triflate counterion ([O$_3$SCF$_3$]$^-$),[16] has been neglected in the force field, since a similar observation has not been reported for another common counterion, [SbF$_6$]$^-$,[18,48] and the inclusion of any loosely coordinated counterions would complicate the force field parametrization significantly.

4
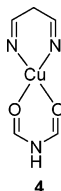
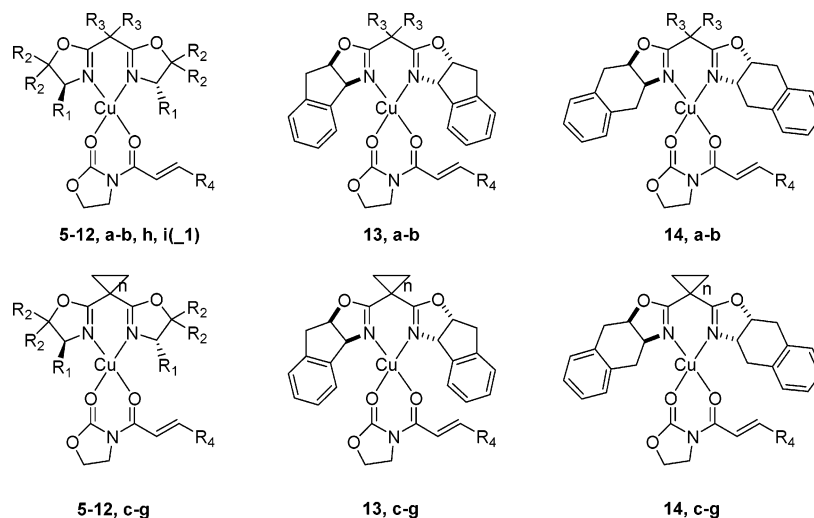While steric interactions favor a tetrahedral arrangement of ligands about a metal center, the electronic stabilization of a d^9 copper(II) center favors a square-planar coordination geometry. Available crystal structures of the aquo complexes of copper(II) bis(oxazolines) display an intermediate structure, which can best be described as a distorted square-planar ligand arrangement.[4,12,17,18,21,48] Gradient-corrected DFT calculations on model complex **4** (described in the Experimental Section) gave rise to a square-planar geometry, thus identifying control of ligand plane twisting (Figure 1) as a key electronic effect important in determining the complex geometry.

This electronic effect was integrated into the parameter set by generation of a DFT-MM difference plot[49] for model complex **3**, where R, R′, R″ = H, followed by analytical fitting of the resulting energy profile (Figure 2) to the torsion potential function $E_{\text{tor}} = \sum |C_n| + \sum C_n (\cos (n\chi))$, with $n = 2$ and χ as defined in Figure 2, to determine a rotational barrier for the observed ligand plane twisting. The DFT-calculated profile showed a very shallow energy minimum centered on $\chi = 10°$, presumably in response to weak steric interactions between the bis(oxazoline) and acrylimide ligands.

To introduce this barrier to ligand plane twisting into the MMFF94 force field, a hidden dummy bond as shown in Figure 3 was introduced to the catalyst$-$substrate complex. [We have also explored a bonding model where the dummy bond is located in the substrate, connecting the copper atom to the acrylimidic nitrogen. This model displayed similar properties and a slightly better reproduction of ligand bite angles in the presence of sterically demanding backbone substituents (vide infra), but the approach described here in detail was pursued to enhance transferability to other Cu(II)-bis(oxazoline)-catalyzed reactions.]

Since MOE does not permit the use of a five-coordinate carbon atom, a new atom type Cx based on a silicon atom was created and associated with existing standard sp^3 carbon parameters. Low force constants were used for parameters involving the dummy bond, with terms chosen to approximate the DFT-calculated geometry of complex **3**. Ideal bond lengths and angles for "real" parameters related to the copper atom were based on available experimental and DFT-calculated data, while force constants were derived from existing parameters. In the absence of a sufficiently large data

Figure 2. Ligand plane twisting energy profiles for model **3** (R, R′, R″ = H).

Table 1. Summary of Complexes Modeled

5-12, a-b, h, i(_1)   13, a-b   14, a-b

5-12, c-g   13, c-g   14, c-g

No.	Substituent (R₁)	R₂ = H, R₄ = H							R₂ = Me, R₃ = Me, R₄ = H	R₂ = H, R₃ = Me, R₄ = Me	double-stereo-differentiation (see part D)
		R₃		n				indane			
		H	Me	1	2	3	4				
5	H	a	b	c	d	e	f		h		*yes* (**5j, k**)
6	Me		b							i	
7	Et		b								
8	¹Pr		b								
9	¹Bu		b						h	i	*yes* (**9j, k**)
10	Ph	a	b	c	d	e	f	g	h	(R₂ = H, **i_1**)	*yes* (**10j, k**)
11	CH₂Ph		b							i	
12	CHPh₂		b								
13	ind[a]	a	b	c	d	e	f	g		i	*yes* (**13j, k**)
14	thn[b]	a	b	c	d	e	f	g			

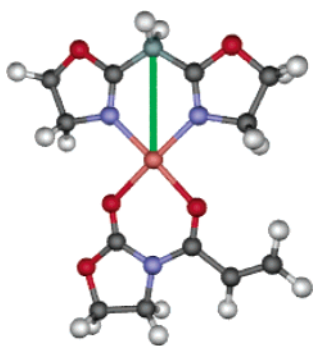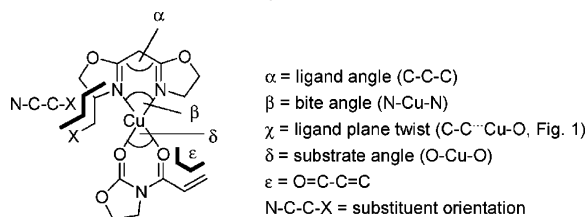[a] Indane. [b] Tetrahydronaphthalene.

Figure 3. Dummy bond model.

set for structural comparison and verification, parameters were not refined beyond these basic approximations. It should also be noted that the same carbon parameters were used for all bis(oxazoline) backbone variations (vide infra), overriding ring-size-specific autotyping by the program. Any parameters added to the MMFF94 default terms are included in the Supporting Information as Table S1.

The resulting MM ligand plane rotational energy profile showed that the fitted parameters underestimate the overall barrier, but reproduction of the energy profile's curvature at small ligand plane twist angles χ resulted in better agreement with available structural data (rms deviation from DFT of 1.86 kcal mol⁻¹ for entire profile, 0.30 kcal mol⁻¹ for range $\chi = 0-60°$). The derived force constant was therefore used without further modification. The relevant ligand plane twist energy plots used for parameter fitting are shown in Figure 2.

B. Catalyst–Substrate Complexes. The force field was verified by comparison of fully optimized MM and DFT structures for **5a–f** (data included in Supporting Information, Table S2), as well as comparison of relevant MM optimized structures with the crystal structures of the catalyst-aquo complexes related to **8–10** (Table 2).[16,18,48,50]

Agreement between DFT- and MM-calculated structural parameters (Table S2) is generally satisfactory, with rms deviations of 0.04 Å, 4.45°, and 3.24° for bond lengths, angles, and torsions, respectively. MM-calcu-

Table 2. Comparison of Selected Structural Parameters for Crystal Structures of Aquo Complexes and MM Optimized Catalyst−Substrate Complexes

α = ligand angle (C-C-C)
β = bite angle (N-Cu-N)
χ = ligand plane twist (C-C···Cu-O, Fig. 1)
δ = substrate angle (O-Cu-O)
ε = O=C-C=C
N-C-C-X = substituent orientation

no.	tN−Cu/Å	α/deg	β/deg	χ/deg	N−C−C−X/deg [a]	ref
(a) Aquo Complex Crystal Structures						
(S,S)Cu-{^{i}Pr-box}	1.97	112.5	91.5	10.2[b]	−58.2	18
$(OH_2)_2(SbF_6)_2$ (cf. **8b**)	1.96				−51.5	
(S,S)Cu-{^{t}Bu-box}	1.91	111.2/113.8	94.0/95.2	42.6/42.7[b]	176.9	17, 48
$(OH_2)_2(SbF_6)_2$ (cf. **9b**)[c]	1.91/1.94				−175.5/179.9	
	1.93				−179.8	
(S,S)Cu-{^{t}Bu-box}	1.92	113.1	94.1	38.0[b]	−177.9	16, 17
$(OH_2)_2(O_3SCF_3)_2$ (cf. **9b**)	1.96				178.9	
(S,S)Cu-{Ph-box}	2.00	112.0	88.9	−12.8[b]	36.3	18
$(OH_2)_2(SbF_6)_2$ (cf. **10b**)	2.00				42.1	
(b) MM Structures of Catalyst−Substrate Complexes[d]						
8b	1.95	114.0	90.9	39.5	173.6	this work
	1.95				173.8	
9b	1.95	114.0	91.1	40.2	−177.6	this work
	1.95				−177.7	
10b	1.95	113.8	90.4	23.2	36.3	this work
	1.95				53.8	

[a] X = H (^{i}Pr), C (^{t}Bu, Ph). [b] Average of both possible χ. [c] Two molecules in unit cell. [d] From 100 iteration stochastic conformational searches.

lated ligand plane twisting angles correspond quite well with the DFT-calculated shallow energy minimum around χ = 10° for the unsubstituted bis(oxazoline) complex (Figure 2). However, the MM force field gives rise to very large ligand internal and bite angles (α and β, respectively) in the presence of sterically demanding cyclopropyl and cyclobutyl backbone substituents (**5c,d**). This may be related to the use of the same backbone parameters independent of ring size, as well as the neglect of electronic effects to counter these distortions. A similar trend, albeit less pronounced, has been observed in the LFMM study of copper(II) bis(oxazoline) aquo complexes.[20]

Comparison of selected structural parameters for the MM optimized catalyst−substrate complexes **8b**−**10b** and the crystal structures of the corresponding catalyst-aquo complexes shows generally good agreement. The main discrepancies arise for the ligand plane twisting angles χ observed for the isopropyl- and phenyl-substituted bis(oxazoline) ligands. The small ligand plane twist angles (χ) observed for phenyl-substituted **10b** may be related to the change in steric demands on replacing the acrylimide substrate with water molecules. This facilitates the closer approach to planar coordination of the smaller water ligands and is thus in good agreement with the broad energy minimum observed for the DFT energy profile of model **3** (Figure 2, R, R′, R″ = H). The change in sign for the aquo complex may likewise be related to the reduced steric interactions between the phenyl substituents on the bis-

(oxazoline) ligand and the coordinated waters, giving rise to a generally shallow potential energy surface (PES) with respect to ligand plane twisting. Intermolecular interactions in the crystal environment could also have reduced ligand plane twisting in the observed structure, which would again be facilitated by a shallow PES. For the isopropyl-substituted **8b**, the different substituent orientations should be noted. The lowest energy structure found in the 100-step stochastic conformational search has both isopropyl substituent hydrogens twisted away from the copper center (∠N−C−C−H = 173.8°/173.8°), hence presenting a substituent profile similar to that of a *tert*-butyl group to the core of the complex. However, two further conformers, one with mixed substituent orientation (∠N−C−C−H = −54.2°/173.9°) and one presenting the sterically least demanding H to the complex core (∠N−C−C−H = −54.3°/−54.3°), may be observed within 0.2 and 0.7 kcal mol^{-1} of the energy minimum, respectively. Given these small energy differences, these conformers would be significantly populated at the reaction temperature (commonly between −78 and +25 °C). The associated ligand plane twist angles χ of 24.0° and 24.9° clearly illustrate the balance of substituent size and ligand plane twisting as well as highlighting the importance of performing conformational searches. Agreement with the average χ = 10.3° observed for the corresponding catalyst-aquo complex is thus improved. The dominant steric influence of the *tert*-butyl substituents in **9b** is expressed as good structural agreement between the acrylimide- and aquo-substituted catalyst complexes.

Figures 4 and 5 show a summary of key structural parameters determined from 100 iteration MM stochastic conformational searches for some of the catalyst−

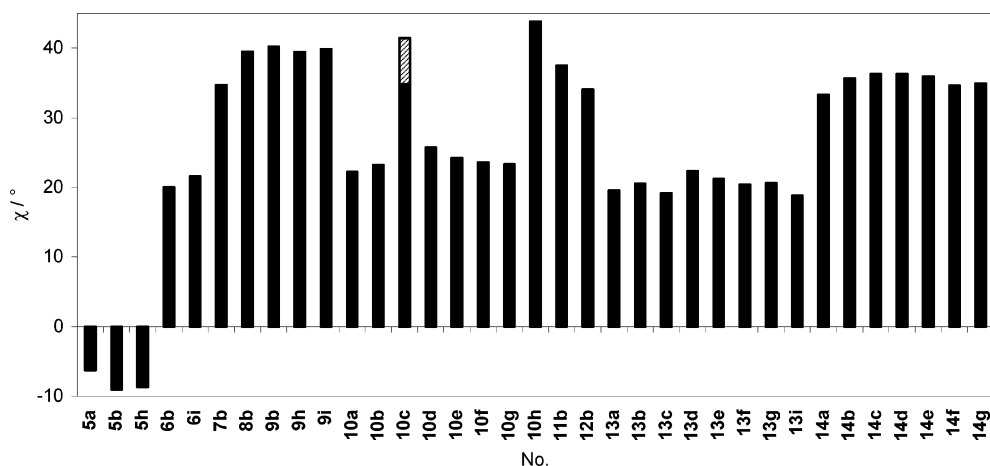(47) Michalak, A.; Ziegler, T. *Organometallics* **2000**, *19*, 1850.
(48) Evans, D. A.; Peterson, G. S.; Johnson, J. S.; Barnes, D. M.; Campos, K. R.; Woerpel, K. A. *J. Org. Chem.* **1998**, *63*, 4541.
(49) Hopfinger, A. J.; Pearlstein, R. A. *J. Comput. Chem.* **1984**, *5*, 486.
(50) Fletcher, D. A.; McMeeking, R. F.; Parkin, D. *J. Chem. Inf. Comput. Sci.* **1996**, *36*, 746.
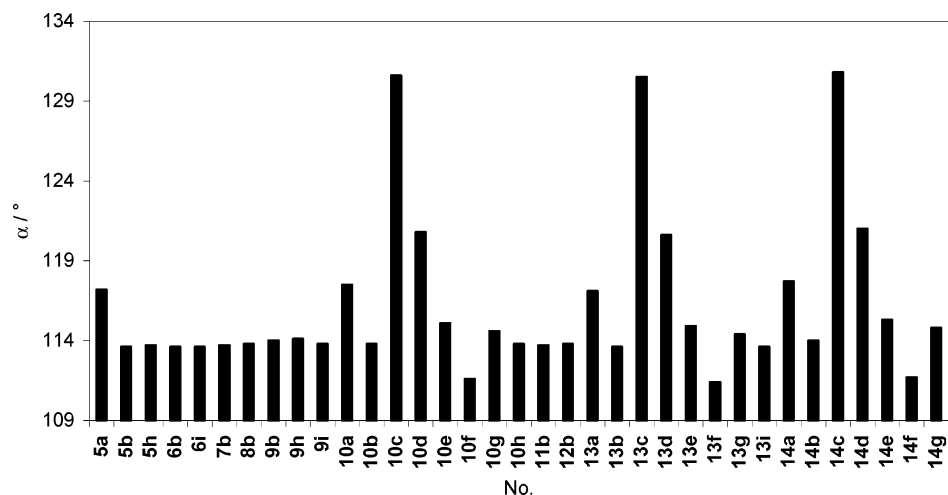
Figure 4. Variation of ligand angle (α) with bis(oxazoline) ligand.


Figure 5. Variation of ligand plane twist angle (χ) with bis(oxazoline) ligand. (Note: **10c**, two energetically equivalent structures).

substrate complexes **5**–**14**. The underlying data have been included in the Supporting Information as Table S3.

Figure 4 confirms the exaggerated response of MM optimized structures to variations in the backbone substituents (vide supra), resulting from the use of carbon parameters independent of ring size. Variation of bis(oxazoline) steric bulk clearly correlates with changes in the values of χ both in the lowest energy conformers (Figure 5) and for Boltzmann population-weighted averages (Table S4). Larger, more three-dimensional substituents generally force larger ligand plane twist angles. The impact of substituent size and shape may be illustrated by comparing the lowest energy conformers of **13b** and **14b**, where the enhanced three-dimensionality of the tetrahydronaphthalene-substituted bis(oxazoline) **14b** gives rise to the larger values of χ observed.

The pronounced response of ligand plane twist angles to bis(oxazoline) substituent variations may be verified from rotational energy profiles, generated by stepwise modification of the ligand plane twist angle followed by partial geometry optimization, keeping the ligand donor atom positions fixed. Catalyst–substrate complexes **5b**, **9b**, **13b**, and **14b** have been chosen as prototypical examples of the bis(oxazoline) ligands investigated, for which substituent conformational freedom is limited,
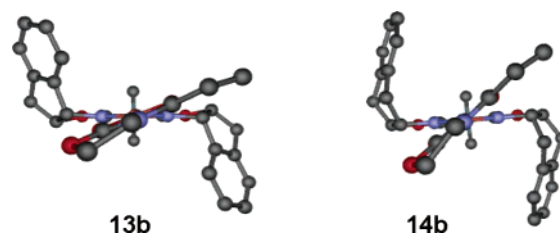
Figure 6. Lowest energy conformers of **13b** and **14b**.

and more detailed exploration of conformational space could thus be neglected. The resulting energy profiles (Figure 7) confirm the energy minima identified from the corresponding conformational search results (Tables S3, S4). Unsubstituted **5b** displays a very shallow energy profile, with a broad minimum at χ = −10°, in agreement with both DFT geometry optimizations and MM conformational searches. In line with observations derived from Figure 6, the indanyl-substituted oxazoline **13b** displays a shallow energy profile with a minimum at χ = 20°, while the more three-dimensional tetrahydronaphthalene group of **14b** gives rise to a slightly steeper profile at low χ and a broad energy mimimum spanning χ = 30–40°. The considerable steric hindrance exerted by the *tert*-butyl substituents of **9b** translates into a steep energy profile with a minimum centered on χ = 40°. A qualitative estimate of the energetic cost
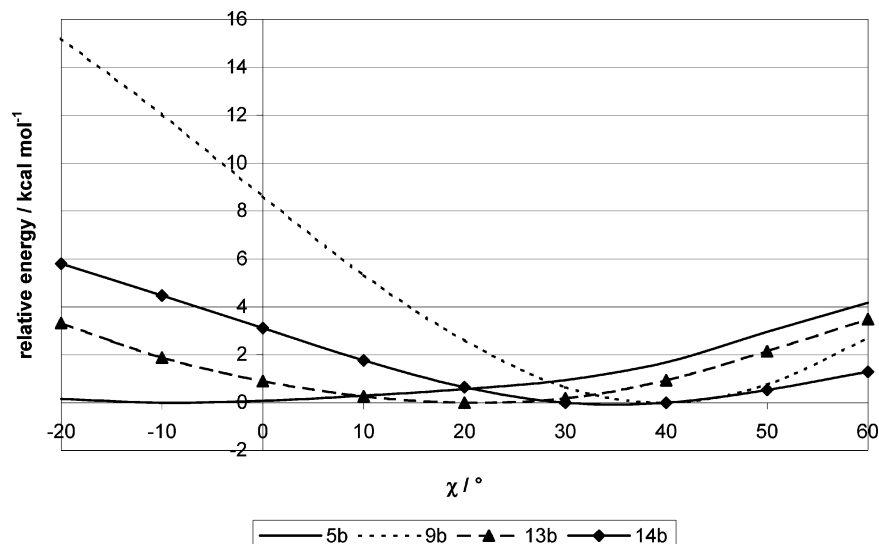
Figure 7. Ligand plane twist angle (χ) rotational energy profiles for catalyst−substrate complexes **5b**, **9b**, **13b**, and **14b**.

of distortion away from the minimum conformation may be gained by inspection of relative energies at 10° above (and below) the minimum. While the shallow energy profiles of **5b** and **13b** cause the energy to increase by only 0.1 (0.2) and 0.2 (0.3) kcal mol⁻¹, respectively, the steeper slopes observed for **9b** and **14b** cause energy increases of 0.8 (0.7) and 0.5 (0.7) kcal mol⁻¹ respectively.

The extent of conformational freedom around the O= C−C=C bond (ϵ) in the acrylimide substrate has also been investigated by generation of rotational energy profiles (Figure S1) for complexes **5b**, **9b**, **13b**, and **14b**. In this case no significant substituent differentiation could be observed, indicating that ligand plane twisting is sufficient to relieve steric strain in these catalyst− substrate complexes. All four profiles show a minimum around $\epsilon = -10°$, and at 10° above (and below) this energy minimum, the energy increases by a maximum of only 0.1 (0.05) kcal mol⁻¹.

Table 3 lists distinct substituent orientations and relative energies for the alkyl- and phenyl-substituted bis(oxazolines) **6b**−**12b** and **10h**. The methyl (**6b**) and *tert*-butyl (**9b**) substituents display the expected C_3-symmetry in their substituent conformational preferences, while both the ethyl (**7b**) and isopropyl (**8b**) groups may be associated with increased conformational variability, in line with the balance between substituent size and ligand plane twist angle (χ) discussed for the isopropyl substituent (vide supra). Similar, but energetically more distinct, conformations may be observed for the bulkier substituents of **11b** and **12b**, where phenyl groups have replaced the methyl substituents of **7b** and **8b**. Especially for **12b**, the increase in steric bulk results in a clear preference for the conformation with the hydrogen atom pointing toward the core of the complex, in contrast to the variability discussed for **8b**. The essentially two-dimensional nature of the phenyl substituents in **10b** gives rise to a number of conformations close in energy, with the partial steric restriction of phenyl rotation in **10h** resulting in a reduction of distinct conformers as well as an increase in energy differences.

C. Reaction Selectivity Predictions. With the structural reliability of the force field as well as sub-

Table 3. Distinct Substituent Orientations (listed according to first occurrence)

| no.	substituent	relative E/kJ mol⁻¹	N−C−C−X1/N−C−C−X2/deg	χ/deg
6b	Me (X = H)	0.00	179/179; 59/59; 179/59	20
		0.05	179/−61; −61/59	20
7b	Et (X = C)	0.00	−69/59	35
		0.73	−171/−69	21
		2.76	59/59	24
		3.43	−171/59	20
		4.58	−171/−171	20
		18.82	−169/179	25
		19.21	−169/−82	29
		19.61	58/179	28
8b	ʲPr (X = H)	0.00	174/174	40
		0.90	174/−54	25
		2.90	−54/−54	25
		4.06	174/62	34
		5.43	62/−54	26
		8.34	62/62	35
9b	ʲBu (X = C)	0.00	−178/−178; 61/−60; 61/61; 61/−178; −60/−178; −60/−60	40
10b	Ph (X = C)	0.00	−145/54; 36/54; 36/−126; −126/−145	23
		0.51	−142/−148	38
		0.77	39/42; −141/42; −141/−139	28
		1.03	34/−140	35
10h	Ph (X = C)	0.00	29/−150; −151/−150; 29/30	44
		3.83	−143/28; −152/37; 28/37	45
		4.41	−146/−151; −146/29	26
		4.44	−152/38	44
		7.46	−145/−142; −142/36; 36/39	25
11b	CH₂Ph (X = C)	0.00	−72/51	37
		2.39	−170/−72	35
		9.92	51/52	26
		11.83	−170/51	23
		14.20	−170/−171	30
12b	CHPh₂ (X = H)	0.00	56/56	34
		3.46	56/−44	22
		14.44	−63/55	30
		14.83	54/−71	54
		15.77	−46/−49	24
		16.44	178/56	36
		19.23	177/−45	19

strate−catalyst complex conformational preferences established, we were interested in determining its performance with respect to regio- and enantioselectivity predictions (Scheme 2). Experimentally, this reaction proceeds with high regioselectivity in favor of *endo* attack and with high enantioselectivity in favor of product P_*n*1, when catalyzed by copper(II) bis(oxazoline) complexes.

Scheme 2
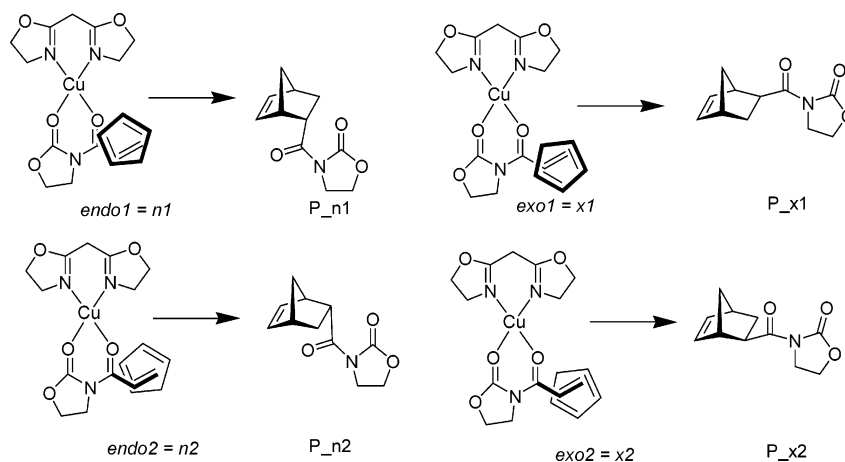
Gradient-corrected DFT linear transit calculations were performed for both possible modes of the experimentally favored *endo* attack of cyclopentadiene on complex **5b** (see Experimental Section for details). At the energy maxima of the respective linear transit paths, geometries were subjected to a full transition state optimization,[51,52] where the converged transition state geometry is identified by a single negative eigenvalue in the Hessian. In line with the shallow energy profile predicted for model **3** (Figure 2, R, R′, R″ = H), several transition state geometries could be identified for both modes of *endo* attack. These were within 1 kcal mol^{-1} of each other and differed mainly in the values calculated for the ligand plane twist χ. As expected for the symmetrical catalyst complex, the lowest energy conformers TS_*n*1 and TS_*n*2 were essentially mirror images of each other, differing by only 0.01 kcal mol^{-1} and with ligand plane twists χ of 29.0° and −29.0°, respectively. These structures have been included in the Supporting Information (Figure S2). As both modes of attack showed similarly asymmetric distances between the dienophile α- and β-carbon atoms and the reacting atoms on the dienophile, a more complete investigation of ligand plane twist conformational freedom was not pursued in this case. The α-C—C distance has been calculated as 2.85 Å, whereas the β-C—C distance is much shorter at 1.71 Å. This observed asymmetry of the diene—dienophile carbon distances in the transition states is in good agreement with previous DFT-calculated transition states for the butadiene and acrolein Diels—Alder reaction.[53] In response to the direction of attack, the transition states display O=C—C=C twisting (ϵ) of similar magnitude, but in opposite directions (TS_*n*1 ϵ = −5.6°, TS_*n*2 ϵ = 5.6°).

Initial inspection suggested that the corresponding catalyst—product complexes might approximate the steric demands of these transition state geometries. However, the calculated energy differences were found strongly in favor of the *exo*-products, with the newly formed bicyclic ring systems often twisting perpendicular to the plane of the complex (Figure 8). Due to this loss of planarity, the catalyst—product complexes differed significantly from the calculated transition state
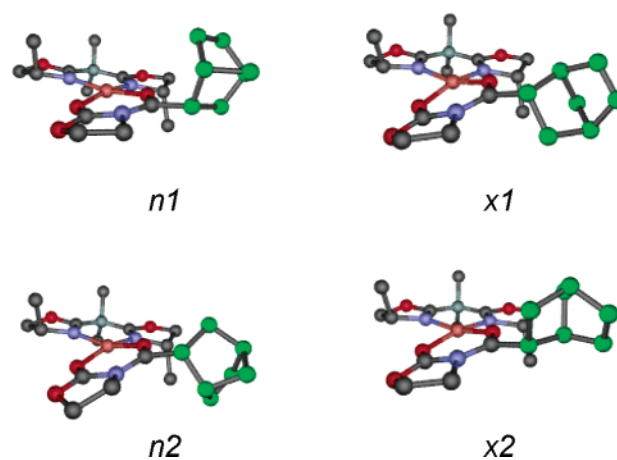
Figure 8. Catalyst—product complexes of **6b** (minima of 100 iteration conformational searches).

geometries and selectivity predictions could not be made.

To avoid the generation of transition state parameters and associated minimizer problems (see for example ref 54 for an early review), the four possible transition state geometries were approximated by a combination of fixed atoms and atom distance restraints (described and validated in the Experimental Section). These transition state geometries were assumed to be transferable, i.e., independent of bis(oxazoline) substituents, thus avoiding extensive transition state searches at the DFT level. Approximate transition states for all four possible modes of attack were used as starting structures for 1000 iteration stochastic conformational searches. Assuming that the calculated energy differences of these transition states correspond to their reactivity, Boltzmann populations could be determined, which were used to assess the regio- and enantioselectivity of different copper(II) bis(oxazoline) complexes. The enantiomeric excesses (ee) predicted for different bis(oxazoline) substituents have been summarized in Table 4, while the corresponding diastereomeric excesses (de) may be found in the Supporting Information (Table S5). Figures 9 and 10 compare available experimental regio- and enantioselectivities with the calculated predictions.

Small energy differences associated with low selectivities are particularly difficult to predict computation-
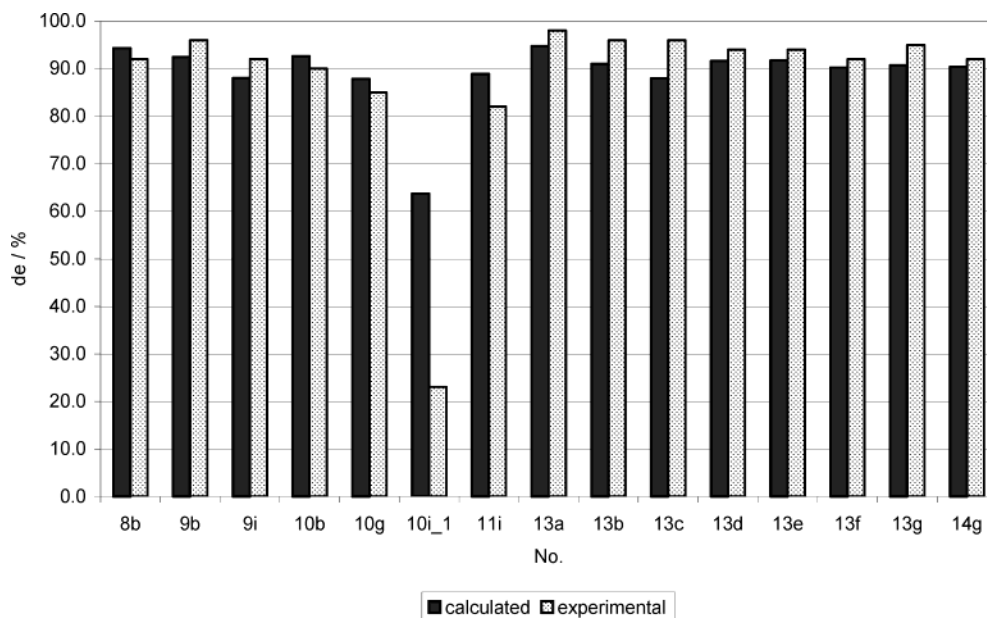
(51) Versluis, L.; Ziegler, T. *J. Chem. Phys.* **1988**, *322*, 88.
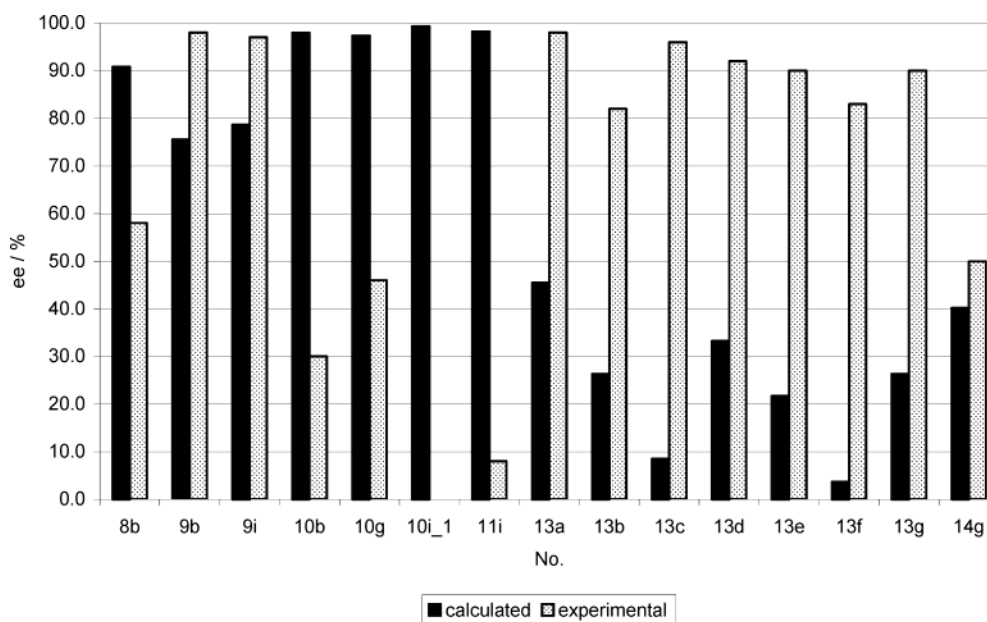(52) Fan, L.; Ziegler, T. *J. Am. Chem. Soc.* **1992**, *114*, 10890.
(53) Kong, S.; Evanseck, J. D. *J. Am. Chem. Soc.* **2000**, *122*, 10418.

(54) Eksterowisz, J. E.; Houk, K. N. *Chem. Rev.* **1993**, *93*, 2439.

Figure 9. Comparison of experimental and calculated regioselectivities (de, %) for bis(oxazoline) ligands.

Figure 10. Comparison of experimental and calculated enantioselectivities (ee, %) for bis(oxazoline) ligands.

ally, so the correctly predicted trend toward reduced regioselectivity for **10h** and **10i_1** is very satisfactory. While *exo* attack is sterically favorable, the major product observed for most Diels−Alder cycloadditions is the result of a more hindered *endo* attack, suggesting kinetic control of the reaction. The standard textbook "rule-of-thumb" explanation attributes this observation to a lowering of the activation energy by secondary orbital interactions between the π-electrons of the diene and unsaturated substituents in the dienophile.[55,56] Since MM force fields by definition neglect such orbital interactions, the predicted regioselectivities are in surprisingly good agreement with available experimental data (Table S5, Figure 9) and suggest that steric factors contribute to the observed regioselectivity.

(55) Isaacs, N. *Physical Organic Chemistry*, 2nd ed.; Longman Group UK Ltd.: Harlow, 1995.
(56) Fleming, I. *Pericyclic Reactions*; Oxford Chemistry Primer No. 67; Oxford University Press: Oxford, 1999.

Table 4. Enantiomeric Excesses (ee) Calculated from MM Transition State Conformational Searches

no.	T/K	calc ee[a]/%	expt ee/%	ref	no.	T/K	calc ee[a]/%	expt ee/%	ref
5a	213	0.6			**11b**	298	50.3		
5b	213	−30.5			**11i**	298	98.3	8	67
5h	213	18.6			**12b**	213	97.4		
6b	213	50.4			**13a**	195	45.5	98.0	7
6i	213	23.3			**13b**	223	26.3	82.5	13
7b	213	22.5			**13c**	223	8.5	96.3	13
8b	195	90.8	58	10	**13d**	223	33.3	92.0	13
9b	195	75.6	>98	10	**13e**	223	21.7	89.5	13
9h	213	79.6			**13f**	223	3.7	83.0	13
9i	258	78.7	97	10	**13g**	223	26.3	89.5	14
10a	213	97.6			**13i**	213	73.7		
10b	195	97.9	30	10	**14a**	213	69.1		
10c	213	96.3			**14b**	213	51.9		
10d	213	92.8			**14c**	213	−52.3		
10e	213	98.9			**14d**	213	55.5		
10f	223	99.9			**14e**	213	66.6		
10g	223	97.4	46.0	14	**14f**	213	−19.5		
10h	298	98.0	10	17	**14g**	223	40.2	49	14
10i_1	298	99.4	0 (n.r.)	67					

[a] Negative values indicate preference for *n*2 transition state; n.r. = near racemic.

We have performed structural analyses of all conformational search results and thus determined Boltzmann population weighted averages of ϵ and χ for all four possible transition states, which have been included in the Supporting Information (Table S6). Weighted ligand plane twisting angles (χ) are generally more similar for the same direction of attack; that is, agreement between the *n*1 and *x*1 transition states, as well as between *n*2 and *x*2, may be observed, and differences in χ can thus be ruled out as the source of regioselectivity. Inspection of the weighted O=C−C=C torsion angles (ϵ) reveals a general trend toward larger values of ϵ for the *exo* modes of attack, but energy profiles generated for rotation about ϵ for the catalyst−substrate complexes (Figure S1) suggest only a small energetic cost for distorting the C=C double bond from coplanarity. The distortion of the *endo* cyclopentadiene (CpH) fragments from planarity is in good agreement with the deformation of the ring system in the DFT-calculated transition state structures (rms distances < 0.1 Å for heavy atom superposition). Determination of the strain energies for the isolated CpH fragments at the relevant transition state conformations shows the *endo* mode of attack to give rise to strain energies between 0.2 and 0.6 kcal mol^{-1} below those of the *exo* transition states. Unfavorable interactions between bis(oxazoline) ligand and hydrogens on the saturated CpH carbon result in a more pronounced distortion of the CpH fragment for the *exo* transition states than for *endo* attacks. The combined energy contributions from O=C−C=C deviation from planarity and the distortion of the cyclopentadiene structure are the main energetic factors in determining regioselectivity.

The prediction of enantioselectivities is less successful with respect to the detailed reproduction of experimental results. The deviation appears to arise from a number of contributing factors:

(a) From the Boltzmann population weighted averages of χ for the different transition state geometries (Table S6), supplemented by the relevant rotational energy profiles for **9b** (Figure S3), the increase in ligand plane twisting in response to unfavorable steric interactions of the reacting site with the bis(oxazoline) substituents observed for the *n*2 (and *x*2) transition state may be identified as the main source of energetic distinction between the *endo* transition states and thus of the predicted enantioselectivities. For steep energy profiles such as **9b**, even small differences in χ give rise to reasonable energy differences and hence enantioselectivity predictions in acceptable agreement with experiment. However, shallow energy profiles as obtained for **13b** and **14b** will be less responsive to changes in χ and hence result in smaller energy differences and reduced selectivities. This highlights the importance of controlling the extent of ligand plane twisting and potentially questions the transferability of the ligand plane twisting parameter to all types of bis(oxazoline) complexes.

(b) Despite the exaggerated effect of backbone variations on the MM optimized geometries, predicted enantioselectivities for the indane and tetrahydronaphthalene bis(oxazoline) ligands are in poor agreement with available experimental data and display no consistent trend in response to structural modifications. In part,

this may be related to the shallow energy profiles observed for the catalyst−substrate complexes **13b** and **14b** (vide supra), but in the absence of further experimental or DFT-calculated structural data, the interdependence of ligand/bite angle and ligand plane twisting is difficult to assess and subtle electronic effects might be important in these cases, which would again affect the transferability of parameters and may not be captured well by a standard MM approach.

(c) Given the importance of asymmetric bis(oxazoline) substituent steric bulk in determining the enantioselectivity imparted by the catalytic system, the assumption that the approximate transition state geometries are fully transferable, i.e., independent of the substituents, should also be questioned. Calculations to validate the definition of transition state geometry used (described in the Experimental Section) have indeed shown that agreement between experimental and calculated enantioselectivities may be improved by slight modifications to the transition state geometry (Table S7). To achieve consistency, DFT transition state searches on fully substituted catalyst complexes rather than a simplified model would have to be undertaken for each group of substituents studied. The energetic reliability of the MM optimized transition states can be tested by performing single-point DFT calculations on the two possible *endo* transition states of **9b** as located by MM conformational searches. While at MM level the *n*2 transition state lies 1.8 kJ mol^{-1} above the *n*1 mode of attack, at DFT level this energy difference increases to 7.1 kJ mol^{-1}, thus improving the predicted enantioselectivity from *n*1:*n*2 = 73:27 to 98:2, if only these two transition state conformations are considered. This rough test suggests that the MM-calculated energy differences underestimate DFT energy predictions. However, given the observed interplay between substituent orientations and ligand plane twisting, a more complete sampling of conformational space would be computationally very expensive, and in the interest of simplicity and versatility of this modeling approach, this has not been pursued further at this stage.

(d) While the expected trend toward an increase in enantioselectivity with substituent steric hindrance may to some extent be observed for the alkyl substituents, the discrepancy for isopropyl (**8b**) and *tert*-butyl (**9b**) substituents is considerable. At least in part this may be related to the isopropyl substituents favoring conformations that remove the sterically less demanding hydrogen atom from the core of the complex, hence increasing steric resemblance to the *tert*-butyl group (vide supra). Assuming full transferability and hence reliability of the underlying original MMFF94 parameter set, restriction of alkyl substituent rotational freedom, e.g., through weak association of counterions or the presence of solvent molecules, might be sufficient to favor conformations with the hydrogen atoms of the isopropyl group turned toward the copper atom, hence reducing χ and predicted enantioselectivities, but these effects have not been considered in this study. Conformational freedom of the phenyl substituents, where enantioselectivity is also overestimated, might likewise be reduced by weak interactions with solvent molecules or counterions, which will be discussed further in section D. [In this case, parameters for rotation about the

Scheme 3

stereochemically matched

stereochemically mismatched
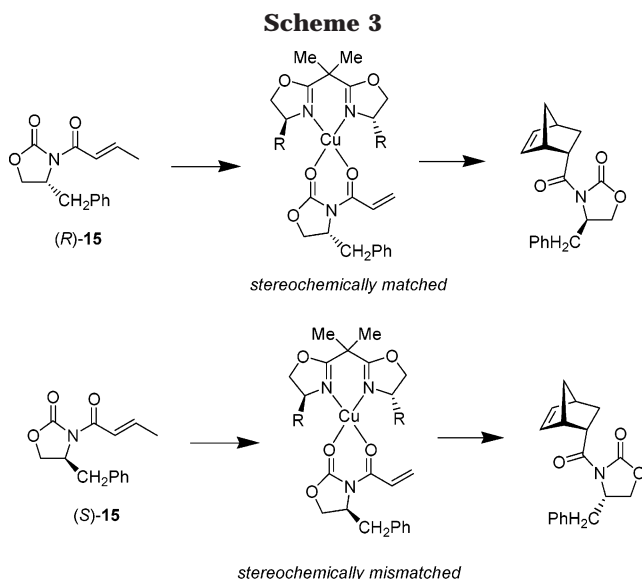
Table 5. Summary of Experimental Data for 9j,k and 10j,k

no.	R =	substrate	T/K	endo:exo	de (%)[a]	ref
9j	^{t}Bu	(R)-**15**	195	99:1	>98	10, 17
9k	^{t}Bu	(S)-**15**	195	97:3	36	10, 17
10j	Ph	(R)-**15**	195	99:1	92	17
10k	Ph	(S)-**15**	195	95:5	−82	17

[a] Based on *n*1:*n*2; negative values indicate preference for *n*2 product.

oxazoline−phenyl C−C bond have been verified by comparison of DFT- and MM-calculated rotational energy profiles for 4-(S)-phenyl-2-oxazoline (rms error = 1.24 kcal mol^{-1} for single-point calculations, with discrepancies mostly for energy maxima).]

D. Double Stereodifferentiation Experiments. While the crystal structures of the catalyst−aquo complexes clearly display a distorted square-planar ligand arrangement about the copper(II) center[16−18,48] and the observed product distribution has been rationalized based on a square-planar catalyst−substrate intermediate (see for example refs 12, 17, 57), its existence in solution has not been directly confirmed from the experimental data. Evans and co-workers have devised a series of double-stereodifferentiation experiments,[17,21,57] where an additional chiral center is introduced to the substrate, giving rise to stereochemically matched and mismatched reactions with respect to the bis(oxazoline) chirality. Reaction of (R)-**15** (Scheme 3) is expected to correspond to the stereochemically matched case for a square-planar complex, whereas a tetrahedral coordination would make this the mismatched case. The opposite is true, if substrate (S)-**15** is used. The experimental results have been summarized in Table 5.

As expected (vide supra), and since confirmed by DFT calculations, the catalyst−substrate complex indeed adopts a distorted square-planar geometry about the copper(II) center. However, an interesting observation from this set of reactions for **9j,k** and **10j,k** is that for the sterically demanding *tert*-butyl-substituted complexes (**9j,k**), the predominant stereochemically mismatched product is determined by the catalyst chirality,

(57) Evans, D. A.; Lectka, T.; Miller, S. J. *Tetrahedron Lett.* **1993**, *34*, 7027.

Table 6. Predicted Regio- (*endo:exo*) and Stereoselectivity (de) Results from Double-Stereodifferentiation Calculations (restr. = restrained geometry)

no.	R =	substrate	endo:exo	de (%)[a]
5j	H	(R)-**15**	95.5:4.5	65.7
5k	H	(S)-**15**	95.1:4.6	−69.9
9j	^{t}Bu	(R)-**15**	95.5:4.1	95.9
9k	^{t}Bu	(S)-**15**	97.8:2.2	64.8
10j	Ph	(R)-**15**	96.7:3.3	100.0
10k	Ph	(S)-**15**	97.1:2.9	94.0
10j	Ph, restr.	(R)-**15**	91.2:8.8	77.4
10k	Ph, restr.	(S)-**15**	97.3:2.7	−9.1
13j	ind	(R)-**15**	97.2:2.8	95.7
13k	ind	(S)-**15**	97.1:2.9	−8.4

[a] Based on *n*1:*n*2; negative values indicate preference for *n*2 product.

whereas the product of the less hindered phenyl-substituted complexes (**10j,k**) is controlled by the dienophile substrate chirality.

To further assess the reasons for the discrepancies between experimental and calculated selectivities for the essentially two-dimensional phenyl and indanyl bis-(oxazoline) substituents, 1000 iteration stochastic conformational searches on the transition state complexes incorporating a chiral substrate along with *tert*-butyl-, phenyl-, and indanyl-substituted bis(oxazolines) **9j,k**, **10j,k**, and **13j,k**, as well as the unsubstituted complex **5j,k**, have been performed. The predicted regio- and enantioselectivities have been summarized in Table 6. In response to the unsatisfactory agreement between calculated and experimental enantioselectivities for phenyl-substituted **10k** (vide infra), conformational searches were repeated with restrained starting geometries, such that the N−C−C−C torsions mimicked the phenyl ring orientation observed in indane bis(oxazoline) ligands (N−C−C−C = 120°, weight 10). (The weighting indicates the proportion by which the total potential energy is increased in response to violation of the target value.) These results have also been included in Table 6.

Predicted regioselectivities are again in good agreement with experimental observations. The results for the unsubstituted complexes **5j,k** confirm that enantioselectivity has been induced by the substrate chirality. Similarly, enantioselectivity for the *tert*-butyl-substituted complexes **9j,k** is controlled by the oxazoline chirality, and predictions are in reasonably good agreement with the experimental data (Table 5). While predictions for the stereochemically matched reaction of **10j** are in good agreement with experiment, the mismatched reaction for **10k** is predicted to be controlled by the oxazoline chirality, indicative of a sterically demanding substituent similar to *tert*-butyl, in contradiction of the experimental data. The results for the indane-substituted bis(oxazoline) complexes **13j,k** correspond to the substrate chirality control expected for a sterically less demanding group and confirm the viability of this double-stereodifferentiation calculation approach for assessing the steric demands of bis-(oxazoline) substituents. When the conformational searches were repeated with the phenyl substituent conformational freedom restrained to geometries resembling the indane, agreement between calculated and experimentally observed enantioselectivities was im-

proved considerably for the stereochemically mismatched case (**10k**). In line with results discussed previously, this may indicate more limited conformational freedom of the phenyl substituents in solution and under reaction conditions, possibly related to interactions with surrounding solvent molecules and counterions. Unrestrained rotation of the phenyl rings turns these into essentially three-dimensional ligands, as confirmed by the double-stereodifferentiation calculations. In the reaction environment this rotation may be more restricted, with the phenyl-substituted bis(oxazoline) ligand resembling the indanyl-substituted ligand in terms of steric demands.

Conclusions

We have presented a comparatively simple extension to the well-known MMFF94 molecular mechanics force field, which permits the computational investigation of substituent effects in bis(oxazoline) copper(II)-catalyzed Diels−Alder reactions between cyclopentadiene and acrylimides, but would also be adaptable to similar catalyst complexes. Conformational preferences of catalyst−substrate complexes and approximate transition states have been investigated and regio- and enantioselectivities have been predicted from conformational search results.

Calculated regioselectivities were in surprisingly good agreement with available experimental data, despite the potential importance of secondary electronic effects in favoring *endo* selectivity as advocated by standard textbooks. This could be linked to the energetic differentiation of *exo* and *endo* transition states derived from a combination of out-of-plane deformation of the dienophile and the more pronounced distortion of the cyclopentadiene in response to unfavorable interactions with the bis(oxazoline) ligands in the *exo* transition states.

The prediction of enantioselectivities, found to arise from differences in ligand plane twisting (χ), was considerably less successful and affected by a number of factors. Given the importance of control over the ligand plane twist angle χ, transferability of the relevant parameter to all types of bis(oxazoline) ligands will need to be investigated further. In addition, prediction of the effect of systematic bite angle variations on enantioselectivity has been very poor and appears to necessitate a more balanced treatment of electronic and steric effects. In some instances, excessive conformational freedom gave rise to an overestimation of enantioselectivities, which could be improved by modification of the original MMFF94 parameter set or a more comprehensive representation of the reaction environment, to include, for example, solvation and counterion coordination. The presence of different counterions in particular has been found to influence reactivity and selectivity in a range of reactions catalyzed by copper(II) bis(oxazoline) complexes, and their steric influence merits further investigation.[17,22,58,59] The analysis of conformational freedom for different bis(oxazoline) catalysts was

supplemented by a series of computational double-stereodifferentiation experiments, which allowed the steric characteristics of key substituents to be determined. While transition state geometries may be affected by the steric requirements of different bis(oxazoline) ligands, the assumption of transition state transferability could also have affected the quality of the calculated enantioselectivity predictions, thus providing a further avenue of investigation. DFT single-point calculations on two MM optimized transition state conformations showed the energy differences to be underestimated at the MM level, thus underlining the need for a more comprehensive treatment of both steric and electronic contributions to predicted selectivity.

We have recently successfully ported the LFMM approach into the molecular operating environment (MOE) used in this investigation.[60] This approach improves the treatment of metal-based electronic effects and can allow for varying metal coordination numbers, while retaining the advantages of a molecular mechanics approach, i.e., permitting extensive conformational searching and molecular dynamics. We plan to develop LFMM parameters suitable for the modeling of these complexes soon and to apply the transition state approximation described here to investigate the scope of a geometrically and electronically flexible molecular mechanics approach for the rational design of transition metal catalysts. Used in conjunction with the results of more detailed DFT calculations, the quality of results achieved from an improved treatment of the metal center should also provide us with an indication of the need for further improvements to the modeling of the transition state.

Experimental Section

A. Density Functional Theory. The DFT calculations were performed using ADF 2000.02[51,61−64] and ADF 2002.03/2003.01[51,52,64−66] on the Chemistry Department's 32 dual-processor Linux cluster at the University of Warwick, using default convergence criteria and the BLYP generalized gradient approximation (GGA) throughout. The BLYP GGA was chosen, as it gave transition state geometries in good agreement with results reported for the Diels−Alder reaction of butadiene and acrolein.[53] All calculations were performed on isolated molecules. Geometry optimizations of model complex **4**, as well as linear transits and transition state searches for the reaction of cyclopentadiene with complex **3** (R, R′′ = H, R′ = Me), used a basis set of triple-ζ quality with one polarization function (basis set IV, TZP) and a 2p frozen core on the copper atom, basis sets of double ζ-quality with one polarization function (basis set III, DZP) and a 1s frozen core for the nitrogen and oxygen donor atoms, and basis sets of double-ζ

(58) Evans, D. A.; Kozlowski, M. C.; Murry, J. A.; Burgey, C. S.; Campos, K. R.; Connell, B. T.; Saples, R. J. *J. Am. Chem. Soc.* **1999**, *121*, 669.

(59) Evans, D. A.; Rovis, T.; Kozlowski, M. C.; Tedrow, J. S. *J. Am. Chem. Soc.* **1999**, *121*, 1994.

(60) Deeth, R. J.; Fey, N.; Foulis, D. L.; Williams-Hubbard, B. J. Publication in preparation.

(61) *ADF 2000.01, Scientific Computing & Modelling NV, Theoretical Chemistry*; Vrije Universiteit: Amsterdam, The Netherlands, 2000, http://www.scm.com.

(62) Baerends, E. J.; Ellis, D. E.; Ros, P. *Chem. Phys.* **1973**, *2*, 41.

(63) te Velde, G.; Baerends, E. J. *J. Comput. Phys.* **1992**, *99*, 84.

(64) Fonseca Guerra, C.; Snijders, J. G.; te Velde, G.; Baerends, E. J. *Theor. Chem. Acc.* **1998**, *99*, 391.

(65) te Velde, G.; Bickelhaupt, F. M.; van Gisbergen, S. J. A.; Fonseca Guerra, C.; Baerends, E. J.; Snijders, J. G.; Ziegler, T. *J. Comput. Chem.* **2001**, *22*, 931−967.

(66) *ADF 2002.03, Scientific Computing & Modelling NV, Theoretical Chemistry*; Vrije Universiteit: Amsterdam, The Netherlands, 2002, http://www.scm.com.

(67) Takacs, J. M.; Quincy, D. A.; Shay, W.; Jones, B. E.; Ross, C. R., III. *Tetrahedron: Asymmetry* **1997**, *8*, 3079.

quality (basis set II, DZ) for all other atoms. Geometry optimizations of complexes **5a**−**f** and all single-point calculations used basis sets of triple-ζ quality with one polarization function (basis set IV,TZP) for all non-hydrogen atoms with a 2p frozen core on the copper atom and 1s frozen cores on all main group elements, while a double-ζ quality basis set (basis set II, DZ) was used for the hydrogen atoms. Single-point energies were calculated from optimized geometries, where the torsion of interest had been modified.

B. Molecular Mechanics. All MM calculations were performed using MOE 2001.01[24] on a standard 1.2 GHz PC, using the MMFF94 force field and default convergence criteria, unless stated otherwise. Calculations were performed on isolated molecules and in the absence of electrostatics; that is, no charges were assigned. The force field was derived and verified as described in part A of Results and Discussion, and any parameters added to the MMFF94 default terms are listed in the Supporting Information (Table S1). Similar to the DFT approach, single-point energies used in the parametrization and for the verification of existing parameter terms were calculated from optimized geometries, where the torsion of interest had been modified. Rotational energy profiles were generated by stepwise modification of the torsion of interest, which was then treated as fixed while allowing full relaxation of the remaining degrees of freedom. Conformational space for the catalyst−substrate complexes was explored by 100 iteration stochastic conformational searches with default settings, except for disabling chiral inversion for structure generation and the automatic calculation of force field charges. Structures within 5 kcal mol^{-1} of the energy minimum were recorded in the output database.

The DFT-calculated transition state structures were approximated by a combination of fixed atoms and atom distance restraints. The shorter β-C−C distance of ca. 1.7 Å could not be achieved by a suitably weighted restraint and necessitated fixing the two atoms at a distance of 1.7 Å in space (in MOE, fixed atoms may not be moved in an optimization and their potential gradients are set to zero). A restraint of 2.85 Å with a weighting factor of 10 was found suitable to achieve a longer α-C−C distance of ca. 2.95 Å. Shorter distances and larger weighting factors were found to impair the minimizer, such that viable convergence gradients could not be reached. This choice of transition state approximation was validated by

systematic variation of both α- and β-C−C distances (steps of 0.1 Å, ranging 1.7−2.0 Å and 2.75−2.95 Å, respectively) in a series of 100 iteration stochastic conformational searches (vide infra for settings) on complexes **5a**, **9b**, **10b**, and **13b**, to determine their impact on predicted enantioselectivities. As discussed in part C of Results and Discussion, agreement with available experimental data might be improved by using different approximations for different bis(oxazoline) ligands, but to maintain transferability, this was not pursued further.

Based on these approximations, transition states structures were generated for all four possible modes of diene attack and were each used as starting structures for 1000 iteration stochastic conformational searches, using the same options as described for catalyst−substrate complexes. However, in this case structures within 10 kcal mol^{-1} of the energy minimum were saved to the database and the rms gradient convergence criterion was increased to 0.1 kcal mol^{-1}. The same setting were used for the validation of the transition state approximations, and several variations were expanded to 1000 iteration stochastic conformational searches for complexes **9b** and **13b** to further investigate the impact of transition state geometry on calculated selectivity.

Supporting Information Available: Tables of force field parameters, calculated structural parameters and diastereoselectivities, the results of extended transition state approximation validations for **10b** and **13b**, and structural coordinates for all DFT optimized complexes and transition states are available as electronic Supporting Information. This material is available free of charge via the Internet at http://pubs.acs.org.

OM0343519